공학석사학위논문

Modeling and Characterization of Magnetoelastic Resonator System for Viscosity Sensing Applications

July, 2015

School of Mechanical & Aerospace Engineering
Seoul National University

Seong-ji Kang

점도 측정 센서를 위한

자기변형 레조네이터의 모델링과 특성 분석

Modeling and Characterization of Magnetoelastic Resonator System for Viscosity Sensing Applications

지도교수 고 상 근

이 논문을 공학석사 학위논문으로 제출함

2015년 7월

서울대학교 대학원

기계항공공학부

강 성 지

강성지의 공학석사 학위논문을 인준함

2015년 7월

위 원 장 _____ 김 민 수 _____ (인)

부위원장 _____ 고 상 근 _____ (인)

위 원 _____ 송 한 호 _____ (인)

Abstract

Modeling and Characterization of Magnetoelastic System for Viscosity Sensing Applicaitions

Seong-ji Kang

School of Mechanical & Aerospace Engineering

The Graduate School

Seoul National University

This paper introduces an equivalent electrical circuit model in air for magnetoelastic resonator system. The whole system are expressed with impedance Z including AC excitation coil, coupling factor, demagnetizing factor, magnetization of material and magnetization. Especially, coupling factor and demagnetizing factor are depicted as a transformer winding ratio η and k respectively.

Also in this paper, an equivalent circuit in viscous loading is introduced. The fact that additional circuit because of surface loading can be added directly to magnetoelastic resonator model without modifying the model is verified by modeling and equation. Furthermore, when various surface loading is applied simultaneously to the magnetoelastic resonator, adding equivalent circuit in series describes the behavior of the resonator.

The case studies based on magnetoelastic resonator operating at several geometries, DC field condition and kinematic viscosity are discussed for verification of suitability of the proposed modeling for describing behavior or magnetoelastic resonator system.

Keywords : Resonator, Magnetoelastic Resonator, Surface Load, Resonance

Student Number : 2013-23051

TABLE OF CONTENTS

LIST OF FIGURES

LIST OF VARIABLES

$\boldsymbol{A}_{\mathbf{reso}}$: cross-sectional area of resonator, m^2

$\boldsymbol{B}$: magnetic flux density, Wb/m^2

$\boldsymbol{C}_{\mathbf{m}}$: capacitance of the motional impedance, *F*

$\boldsymbol{C}_{\mathbf{m'}}$: capacitance of the motional impedance under surface loading, *F*

$\boldsymbol{C}_{\boldsymbol{m}}^{\boldsymbol{k}}$: capacitance divided by $\mathbf{k}^{\mathbf{2}}$ of the motional impedance under surface loading, *F*

$\boldsymbol{C}_{\mathbf{nl}}$: capacitance of Newtonian fluid, *F*

$\boldsymbol{D}$: internal damping of resonator, $N/kg \cdot m^2$

$\boldsymbol{D}_{\boldsymbol{eddy}}$ eddy current loss, $N/kg \cdot m^2$

$\boldsymbol{D}_{\mathbf{0}}$: internal damping of resonator, $N/kg \cdot m^2$

$\boldsymbol{d}$: linear coefficient of magnetostriction arises from magnetization, m/A

$\boldsymbol{E}_{\mathbf{H}}$: effective Young's modulus of resonator at constant field, N/m^2

$\boldsymbol{E}_{\mathbf{M}}$: effective Young's modulus of resonator under magnetically free condition, N/m^2

$\boldsymbol{e}_{\boldsymbol{tot}}$: the sum of the elastic strain

$\boldsymbol{F}_{\boldsymbol{damping}}$: damping force of resonator, N

$\boldsymbol{F}_{\boldsymbol{elastic}}$: elastic force of resonator, N

$\boldsymbol{F}_{\boldsymbol{inertial}}$: inertial force of resonator. N

$\boldsymbol{H}$: magnetic field applied to the resonator ($\boldsymbol{H} = \boldsymbol{H}_{\mathbf{ac}} + \boldsymbol{H}_{\mathbf{dc}}$), A/m

$\boldsymbol{h}$: thickness of the resonator, m

$\boldsymbol{k}^{\mathbf{2}}$: magnetoelastic coupling factor

$\boldsymbol{L}_{\mathbf{coil}}$: inductance of the solenoid coil, H

$\boldsymbol{L}_{\mathbf{m}}$: inductance of the motional impedance, H

$\boldsymbol{L}_{\mathbf{m'}}$: inductance of the motional impedance under surface loading, H

$\boldsymbol{L}_{\boldsymbol{m}}^{\boldsymbol{k}}$: inductance divided by $\mathbf{k}^{\mathbf{2}}$ of the resonator arisen from magnetization, H

$\boldsymbol{L}_{\boldsymbol{mg}}$: inductance of the resonator arisen from magnetization, H

$\boldsymbol{l}$: longitudinal length of solenoid coil, m

$\boldsymbol{\Delta l}$ **:** change of longitudinal length of solenoid coil, m

$\boldsymbol{M}$: Magnetization of resonator, A/m

$\boldsymbol{M}_{\mathbf{ac}}$: Magnetization of resonator due to AC excitation magnetic field, A/m

$\boldsymbol{M}_{\mathbf{dc}}$: Magnetization of resonator due to DC bias magnetic field, A/m

$\boldsymbol{M}_{\mathbf{s}}$: Magnetization of resonator under magnetically saturated condition, A/m

$\boldsymbol{N}$: number of turns of the solenoid coil

$\boldsymbol{Q}$: quality factor

$\boldsymbol{R}_{\mathbf{m}}$: resistance of the motional impedance, Ω

$\boldsymbol{R}_{m'}$: resistance of the motional impedance under surface loading, Ω

$\boldsymbol{R}_{m}^{k}$: resistance divided by $\mathbf{k}^{2}$ of the motional impedance , Ω

$\boldsymbol{R}_{\mathbf{nl}}$: resistance of Newtonian fluid, Ω

$\widetilde{\boldsymbol{R}_{s}}$: real term of mechanical impedance of the resonator

$\boldsymbol{T}_{\mathbf{xy}}$: shear surface loading per unit area, N/m^2

$\boldsymbol{u}$: displacement of the resonator, m

$\boldsymbol{V}$: voltage, V

$\widetilde{\boldsymbol{X}_{s}}$: imaginary term of mechanical impedance of the resonator, Ω

$\boldsymbol{Z}_{\mathbf{coil}}$: impedance of ac excitation coil, Ω

$\boldsymbol{Z}_{\mathbf{mg}}$: electrical impedance of the resonator arisen from magnetization, *Ω*

$\boldsymbol{Z}_{\mathbf{ms}}$: electrical impedance of the resonator due to magnetostriction, Ω

$\boldsymbol{Z}_{\mathbf{reso}}$: total electrical impedance of the resonator, Ω

$\boldsymbol{Z}_{\mathbf{sys}}$: total electrical input impedance of network system, Ω

$\widetilde{\boldsymbol{Z}_{s}}$: mechanical impedance of the resonator, Ω

$\boldsymbol{\beta}$: complex wave number

$\boldsymbol{\delta}$: decay length of fluid, mm

$\boldsymbol{\chi}_{\boldsymbol{\sigma}}$: magnetic differential susceptibility of resonator under constant stress $\boldsymbol{\sigma}$

$\boldsymbol{\Phi}$: magnetic flux, Wb/turn

$\boldsymbol{\eta}$: winding ratio of transformer $\mathbf{T_1}$

$\boldsymbol{\eta}_{\boldsymbol{l}}$: dynamic viscosity of fluid, Pa·s

$\boldsymbol{\lambda}$: magnetostriction

$\boldsymbol{\lambda}_{\mathbf{ac+dc}}$: magnetostriction under ac field and dc field

$\boldsymbol{\lambda}_{\mathbf{dc}}$: magnetostriction under dc field

$\boldsymbol{\lambda}_{\mathbf{s}}$:magnetostriction of the resonator under magnetically saturated condition

$\boldsymbol{\mu}_{\mathbf{0}}$: vacuum permeability, $\boldsymbol{\mu}_{\mathbf{0}} = \mathbf{4\pi \times 10^{-7} H/m}$

$\boldsymbol{v}_{\boldsymbol{x}}$: velocity of x-direction, m/s

$\boldsymbol{v}_{\boldsymbol{s}}$: velocity of sensor, m/s

$\boldsymbol{\rho}_{\boldsymbol{el}}$: electrical resistivity, kg/m^3

$\boldsymbol{\rho}_{\boldsymbol{reso}}$: density of the resonator, kg/m^3

$\boldsymbol{\sigma}$: stress applied to the resonator, N/m^2

$\boldsymbol{\omega}$: angular vibration frequency of the resonator, rad/s

$\boldsymbol{\omega_0}$: angular resonant frequency of the resonator, rad/s

$\boldsymbol{\omega_0'}$: shifted angular resonant frequency of the resonator, rad/s

CHAPTER 1.
INTRODUCTION

Resonator system, especially Piezoelectric and Magnetoelastic resonator, is commonly used in Sensor/Actuator nowadays. In this system, physical parameters are measured through observing resonance changes in magnetoelastic resonator due to changes in surroundings [1] [2] [3]. In case of magnetoelastic resonator, exerting time-varying magnetic field on magnetoelastic resonator produces mechanical vibration, enabling measurement of surrounding environment. Because magnetoelastic resonators have distinctive features including temperature stability and remote-querying, they are tremendously advantageous where an electrical contact with the sensing module is not feasible. Therefore, magnetoelastic resonators are applicable in various fields including chemical detections and mechanical property measurements [4]. There are many studies lately on magnetoelastic resonators, of whom most of them are still on their basic level. Some papers present typical data and focus merely on accuracy of the data while other papers propose simple modeling of the system. Nevertheless, these papers does not discuss how the modeling is derived. In this paper, comprehensive system modeling using magnetostriction and h-parameter is proposed. Then the modeling is verified through data comparison.

CHAPTER 2.
MAGNETOSTRICTION

Magnetostriction is the most important concepts in this paper. In this chapter, underlying principles of magnetostriction is discussed. The discussion begins with definition and deriving the principle correlation of magnetostriction. And then these relationships are used to define ΔE effects and coupling coefficient which also is important.

2.1. Magnetostriction of Ferromagnetic Material

Magnetostriction is a property of ferromagnetic material that causes them to deform their dimensions and shape by applied magnetic field [5]. Magnetically induced strain is represented as λ and it is a function of length of material, l:

$$\lambda = \frac{\Delta l}{l} \tag{2.1}$$

When magnetic field is applied to a ferromagnetic material, the material is magnetized. And applied magnetic field force the material to rotate towards a parallel direction with the applied field. If we assume that the magnetostriction is isotropic inside the resonator, magnetically induced strain is simplified to one of a single constant:

$$\lambda(\theta) = \frac{3}{2}\lambda_s\left(\cos^2\theta - \frac{1}{3}\right) \tag{2.2}$$

where θ measures the angle between the direction of the measured magnetostriction and the direction of the saturation magnetization vector. And λ_s means the strain in

saturation. The net magnetization is related to the cosine of the same angle, so magnetizations is expressed in following equation.

$$M = M_s cos\theta \tag{2.3}$$

Combine Eq. (2.2) and Eq. (2.3), magnetostriction becomes:

$$\lambda = \frac{3}{2}\lambda_s\left(cos^2\,\theta - \frac{1}{3}\right) = \frac{3}{2}\lambda_s\left(\left(\frac{M}{M_s}\right)^2 - \frac{1}{3}\right) \tag{2.4}$$

The magnetoelastic resonator operate under a DC biased condition, so the total magnetization is expressed in the following form:

$$M = M_{dc} + M_{ac}e^{jwt} \tag{2.5}$$

The initial magnetization M_i becomes the biased level of magnetization M_{dc}, and the final magnetization M_f represented from Eq. (2.5).

Then, magnetostriction under DC bias field and AC magnetic field is described as:

$$\begin{aligned}\lambda = \lambda_{ac+dc} - \lambda_{dc} &= \frac{3}{2}\lambda_s\frac{\left(M_{dc} + M_{ac}e^{j\omega t}\right)^2 - M_{dc}^2}{M_s^2} \\ &= \frac{3}{2}\lambda_s\frac{2M_{dc}M_{ac}e^{j\omega t} + \left(M_{ac}e^{j\omega t}\right)^2}{M_s^2}\end{aligned} \tag{2.6}$$

subscript dc and ac stands for magnetization from DC and AC magnetic field, respectively. Because AC magnetization M_{ac} is much smaller than M_{dc}($M_{ac} \gg M_{dc}$), magnetostriction in Eq. (2.6) can be approximated as.

$$\lambda \cong 3\lambda_s\frac{M_{dc}M_{ac}e^{j\omega t}}{M_s^2} \cong \left(3\lambda_s\frac{M_{dc}}{M_s^2}\right)M_{ac}e^{jwt} \tag{2.7}$$

Then linear coefficient of magnetostriction d due to magnetization M_{dc} becomes:

$$d = \left.\frac{\partial \lambda}{\partial M}\right|_{dc} = 3\lambda_s \frac{M_{dc}}{M_s^2} \tag{2.8}$$

2.2. ΔE Effect

Magnetoelastic resonance sensors depend on megnetostrictive strain to stimulate vibration, but also rely on the inverse effect where the stress due to vibration yields a change in the magnetic flux. The inverse effect of Joule magnetostriction is known as Villary effect. Le Chatelier's principle describe the relation between Joule and Villary effects through a thermodynamic equation. Le Chatelier's principle is:

$$\left(\frac{\partial \lambda}{\partial \mathrm{H}}\right)_{\sigma} = \mu_0 \left(\frac{\partial M}{\partial \sigma}\right)_{\mathrm{H}} \tag{2.9}$$

where μ_0, σ, is permeability constant, the applied stress respectively. The total strain may be written as the sum of the mechanical strain and the megnetostrictive strain.

$$e_{tot} = \frac{\sigma}{E_M} + \frac{3}{2}\lambda_s \left(\frac{M^2}{M_s^2} - \frac{1}{3}\right) \tag{2.10}$$

And derivative of strain by stress on the resonator can be written in forms of [6]:

$$\frac{\partial e_{tot}}{\partial \sigma} = \frac{1}{E_H} = \frac{1}{E_M} + 3\lambda_s \frac{M}{M_s^2}\frac{\partial M}{\partial \sigma} \tag{2.11}$$

Also derivative of the magnetization by stress on the resonator is by following Villary effect:

$$\frac{\partial M}{\partial \sigma} = \frac{1}{\mu_0}\frac{\partial e}{\partial H} = \frac{3\lambda_s}{\mu_0}\frac{M}{M_s^2}\frac{\partial M}{\partial H}\Big|_{\sigma} = \frac{3\lambda_s}{\mu_0}\frac{M}{M_s^2}\chi_{\sigma} \tag{2.12}$$

And χ_{σ} is a differential susceptibility at constant stress that represents the derivative of the magnetization with the applied magnetic field.

$$\frac{1}{E_H} = \frac{1}{E_H} + 3\lambda_s \frac{M}{M_s^2}\left(\frac{3\lambda_s}{\mu_0}\frac{M}{M_s^2}\chi_\sigma\right) = \frac{1}{E_M} + \frac{9\lambda_s^2}{\mu_0}\frac{M^2}{M_s^4}\chi_\sigma \tag{2.13}$$

Rearranging equation (2.13) by using linear magnetostriction constant d, Eq. (2.8)

$$E_M = E_H + E_H E_M \left(3\lambda_s \frac{M}{M_s^2}\right)^2 \frac{\chi_\sigma}{\mu_0} \tag{2.14}$$

$$\frac{\Delta E}{E} = \frac{E_M - E_H}{E_M} = E_H \frac{d^2 \chi_\sigma}{\mu_0} \tag{2.15}$$

Eq. (2.15) shows that the modulus of elasticity is changeable due to magnetization level. It means that the amplitude of a sensor response is also related to magnetization field. This phenomenon is called "ΔE Effect".

2.3. Magnetoelastic Coupling Factor

There have been a number of properties which have been concerned with the magnetic materials. Magnetoelastic coupling factor k^2 is one of them. Magnetoelastic coupling factor is defined as the ratio of the mechanical energy to the input magnetic energy [7].

$$k^2 \equiv \frac{Elastic\ Energy\ Output}{Magnetic\ Energy\ Input} \tag{2.16}$$

If magnetoelastic coupling factor is high, the conversion is elastic energy into magnetic energy, and vice versa, can be easily achieved [8]. So high magnetoelastic coupling factor means high efficiency. Magnetoelastic coupling factor is expressed in form as [9]:

$$k^2 = 1 - \frac{E_H}{E_M} = \frac{\Delta E}{E_M} = \frac{d^2 E_H}{\mu_0} \chi_\sigma \tag{2.17}$$

From Eq. (2.8), k^2 is also explained as following:

$$k^2 = \left(3\lambda_s \frac{M_{dc}}{M_s^2}\right)^2 \frac{E_H \chi_\sigma}{\mu_0} = E_H \frac{d^2 \chi_\sigma}{\mu_0} \tag{2.18}$$

Eq. (2.18) is equal to the definition of the ΔE effect so that we may use the ΔE effect as a way to determine the amount of coupling in the ferromagnetic material.

CHAPTER 3.
MAGNETOELASTIC RESONATOR MODELING

3.1. Motion of Magnetoelastic Resonator

Figure 3.1 describes the geometry and equation of motion of the resonator.

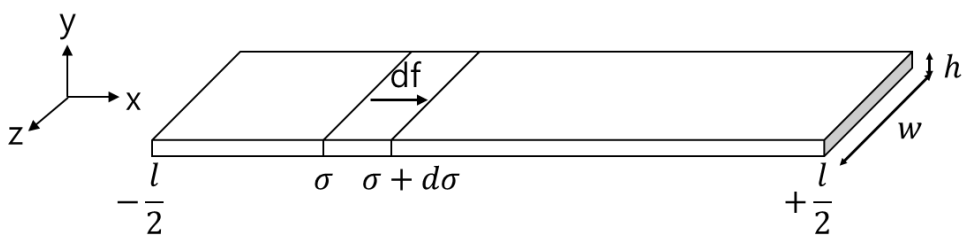

Figure 3.1. Geometry and equation of motion of a resonator.

Before the deviation of motion, the three-dimensional equation of motion is so complicated, therefore the resonator system need assumption. First, the resonator may be simplified to one-dimensional resonator because the thickness of resonator is much less than the length. Actually, the sensor used in this paper is 2826MB (Fe –based ferromagnetic alloy) and its thickness is 30 μm which is much smaller than the length of resonator. Second assumption is that the elastic waves are purely longitudinal. That is, the oscillations are parallel to the direction of x-axis. Then, a one-dimensional equation of motion is derived by relating the elastic force, damping force, inertial force.

Since the inertial stress at specific position is a function of the strain and the modulus elasticity, the inertial stress is expressed as following:

$$\sigma = E_H \frac{\partial u}{\partial x} \tag{3.1}$$

If the stress change is approximated as $\frac{\partial \sigma}{\partial x} dx$, then the elastic force is:

$$F_{elastic} = A(\sigma + d\sigma - \sigma) = A_{reso} d\sigma = A_{reso} \frac{\partial \sigma}{\partial x} dx = E_H A_{reso} \frac{\partial^2 u}{\partial x^2} dx \tag{3.2}$$

Where A_{reso} is area of resonator. Because viscous damping force is generally proportional to the velocity of an object, viscous damping force is described as:

$$F_{damping} = -\left(D_0 \frac{\partial u}{\partial t}\right)(\rho_{reso} A_{reso} dx) = -D_0 \rho_{reso} A_{reso} dx \frac{\partial u}{\partial t} \tag{3.3}$$

Where ρ_{reso} is density of resonator. Another important damping element is eddy current loss. Because the sensor is conductive and magnetic flux is function of time, eddy current loss is important element to consider. The eddy current loss is calculated as following equation:

$$D_{eddy} = \left[\frac{(\pi h)^2}{6\rho_{el}} f_r \mu_0 \chi_\sigma\right] k^2 \tag{3.4}$$

where ρ_{el} represents the electrical resistivity. So the total damping becomes:

$$D = D_0 + D_{eddy} = D_0 + \left[\frac{(\pi h)^2}{6\rho_{el}} f_r \mu_0 \chi_\sigma\right] k^2 \tag{3.5}$$

Next, the inertial component is well known as:

$$F_{inertial} = m\ddot{u} = \rho_{reso} A_{reso} dx \frac{\partial^2 u}{\partial t^2} \tag{3.6}$$

Assuming the resonator as free-free beam, the corresponding equation of motion is:

$$\frac{E_H}{\rho_{reso}} \frac{\partial^2 u}{\partial x^2} + D \frac{\partial u}{\partial t} = \frac{\partial^2 u}{\partial t^2} \tag{3.7}$$

General solution of Eq. (3.7) is:

$$\mathrm{u(x,t)} = [u_1 \cos(\beta x) + u_2 \sin(\beta x)]e^{jwt} \tag{3.8}$$

Because the resonator is assumed as free-free beam, Eq. (3.8) is simplified as below:

$$\mathrm{u(x,t)} = u_2(\sin \beta x)e^{jwt} \tag{3.9}$$

Eq. (3.9) is the general solution of the Eq. (3.7). Since the resonator is assumed as free-free beam, total deformation of the resonator throughout the x-axis is zero.

$$\int_{-l/2}^{+l/2} u(x,t)dx = 0 \tag{3.10}$$

Because the resonator is free-free beam with no external force, stress is also zero at each end.

$$\sigma|_{\pm l/2} = E_H\epsilon - E_H d\chi_\sigma H = 0 \tag{3.11}$$

$$\epsilon = \left.\frac{\sigma}{E_H}\right|_{\pm l/2} = \left.\frac{\partial u}{\partial x}\right|_{\pm l/2} = d\chi_\sigma H = 0 \tag{3.12}$$

Applying above boundary conditions and general solution to the equation of motion Eq. (3.7) gives specific solution:

$$u(x,t) = \frac{d\chi H}{\beta \cos\left(\pm \beta l/2\right)} sin(\beta x)e^{j\omega t} \tag{3.13}$$

Magnetization M may be deducted from the strain and applied magnetic field.

$$M = \frac{\partial M}{\partial e}e + \frac{\partial M}{\partial H}H = \frac{\partial M}{\partial \sigma}\frac{\partial \sigma}{\partial e}e + \frac{\partial M}{\partial H}H \tag{3.14}$$

And applying Eq. (2.12) to Eq. (3.14), then magnetization becomes:

$$M = \frac{d\chi_\sigma}{\mu_0} E_H e + \chi_\sigma H \tag{3.15}$$

Because e is expressed as $\partial U/\partial x$, magnetization is:

$$M = \chi_\sigma H + \frac{d\chi_\sigma E_H}{\mu_0}\frac{\partial u}{\partial x} = \chi_\sigma H + \frac{d^2\chi_\sigma^2 E_H}{\mu_0}\frac{\cos(\beta x)}{\cos\left(\frac{\beta l}{2}\right)} H \tag{3.16}$$

$$M = \int_{-l/2}^{l/2} dM = \chi_\sigma H l \left[1 + 2\frac{k^2}{\beta l} tan\left(\frac{\beta l}{2}\right)\right] \tag{3.17}$$

And the total flux inside the coil is:

$$\Phi = A\mu_0(H + M) = A_c\mu_0 H + A\mu_0\chi_\sigma H l \left[1 + k^2\frac{2}{\beta l} tan\left(\frac{\beta l}{2}\right)\right] \tag{3.18}$$

Where A_c is area of coil, A means the cross-sectional area of resonator. The voltage across the solenoid may be calculated:

$$V = j\omega N\Phi = j\omega N A_c\mu_0 H + j\omega N A\mu_0\chi_\sigma H \left[1 + k^2\frac{2}{\beta l} tan\left(\frac{\beta l}{2}\right)\right] \tag{3.19}$$

Because the H is $(N/l_c)i$, impedance of the resonator system is expressed as:

$$Z_{sys} = j\omega L_{coil} + j\omega L_{coil}\frac{A_{reso}}{A_{coil}} l\chi_\sigma \left[1 + k^2\frac{2}{\beta l} tan\left(\frac{\beta l}{2}\right)\right] \tag{3.20}$$

And rearrange Eq. (3.20), impedance of resonator Z_{reso} is

$$Z_{reso} = \left(Z_{sys} - Z_{coil}\right)/\eta^2 = j\omega N^2 A_{reso}\mu_0\chi \left[1 + k^2\frac{2}{\beta l}\tan\left(\frac{\beta l}{2}\right)\right] \tag{3.21}$$

In Eq. (3.21), Z_{reso} is considered as summation of two parts, which is impedance due to magnetization of resonator and arisen from magnetostriction.

$$Z_{reso} = Z_{mg} + k^2 Z_{ms}. \tag{3.22}$$

Where

$$\begin{aligned} Z_{mg} = j\omega N^2 A_{reso}\mu_0\chi &= j\omega\mu_0 \frac{N^2 A_{coil}}{l}\frac{l\chi}{A_{coil}} A_{reso} \\ &= j\omega L_{coil}\frac{A_{reso}}{A_{coil}} l\chi = j\omega L_{mg}. \end{aligned} \tag{3.23}$$

$$Z_{ms} = j\omega N^2 A_{reso}\mu_0\chi \frac{2}{\beta l}\tan\left(\frac{\beta l}{2}\right) = L_{coil}\frac{A_{reso}}{A_{coil}} l\chi \frac{2}{\beta l}\tan\left(\frac{\beta l}{2}\right) \tag{3.24}$$

$$\begin{aligned} Z_{reso} = Z_{mg} + k^2 Z_{ms} &= j\omega L_{mg}\left[1 + k^2\frac{2}{\beta l}\tan\left(\frac{\beta l}{2}\right)\right] \\ &= j\omega L_{mg} + k^2 j\omega L_{mg}\frac{2}{\beta l}\tan\left(\frac{\beta l}{2}\right) \equiv j\omega L_{mg} + k^2 Z_{ms} \end{aligned} \tag{3.25}$$

Using a first order approximation of the tangent function $\frac{2}{\beta l}\tan\left(\frac{\beta l}{2}\right)$, Z_{reso} is rearranged as follows:

$$\begin{aligned} Z_{reso} &= j\omega L_{mg}\left[1 + k^2\frac{2}{\beta l}\tan\left(\frac{\beta l}{2}\right)\right] \\ &\cong j\omega L_{mg}\left[1 + k^2\frac{4\omega_0^2}{\pi^2}\frac{1}{D^2/4 - jD\omega - \omega^2 + j\,D/2\,\omega_0 + \omega\omega_0}\right] \end{aligned} \tag{3.26}$$

Near the resonant frequency ($\omega \approx \omega_0$), Eq. (3.26) is simplified as follows.

$$Z_{reso} \cong j\omega L_{mg} + k^2\left(\frac{1}{R_m^k} + \frac{1}{j\omega L_m^k} + j\omega C_m^k\right) \tag{3.27}$$

Where

$$L_m = k^2 L_m^k = k^2 L_{mg}\frac{8}{\pi^2} \tag{3.28}$$

$$R_m = k^2 R_m^k = \frac{1}{DC_m} = k^2\frac{\omega_0^2 L_{mg}}{D}\frac{8}{\pi^2} \tag{3.29}$$

$$C_m = k^2 C_m^k = \frac{1}{\omega_0^2 L_m} = k^2\frac{1}{\omega_0^2 L_{mg}}\frac{\pi^2}{8} \tag{3.30}$$

3.2. Equivalent electrical circuit of system

The total system is specified in previous section. In this section, total system is represented in equivalent electrical circuit based on section 3.1.

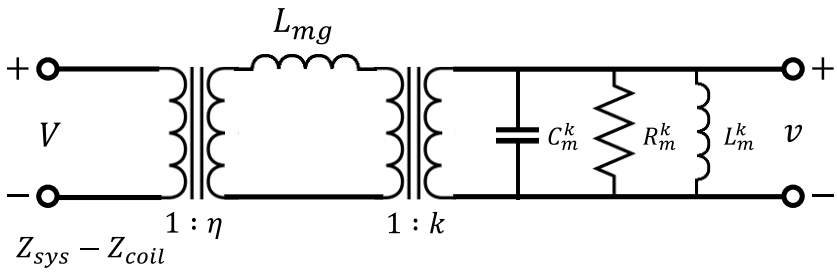

Figure 3.2. Equivalent electrical circuit of system

Figure 3.2 is the Equivalent circuit of total resonator system. There are three parts which are consist of inductance of coil, inductance which is related with magnetization of resonator and magnetostriction of resonator.

The modeling mainly focus on the resonator, inductance of coil is expressed in form of $\mathrm{Z_{sys}} - \mathrm{Z_{coil}}$. In Eq. (3.21), η is converted to transformer ratio to 1: η. η contains many factors such as Demagnetizing factor and AC susceptibility loss. But these factors are negligible, therefore η is considered to 1. Coupling coefficient k in Eq. (3.22) is also converted to transformer ratio to 1: k like impedance changer. And magnetostriction of resonator can be expressed in form of parallel electrical circuit.

CHAPTER 4.
MAGNETOELASTIC RESONATOR UNDER SURFACE LOADING CONDITION

4.1. Mechanical impedance

The mechanical impedance at a given point in a system is the ratio of the sinusoidal force applied to the system at that point to the velocity at the same point. The mechanical impedance of the system $\widetilde{Z_s}$ is given by [10] [11]

$$\widetilde{Z_s} = \frac{T_{xy}}{v_x} = \widetilde{R_s} + j\widetilde{X_s} \tag{4.1}$$

where T_{xy} is the sinusoidal shear stress. v_x is the x-direction velocity. Because the force imposed force is a sinusoidal driving force and velocity is also sinusoidal velocity, the mechanical impedance is combination of the real and imaginary parts like Eq. (4.1).

There are many surface loading types that can be applied to the resonator such as ideal mass loading, Newtonian fluid loading and viscoelastic loading, but Newtonian fluid loading is only considered in this paper.

4.2. Newtonian Fluid

A shear stress in a Newtonian fluid is proportional to the gradient in fluid velocity. So the shear stress imposed by the resonator surface is defined to:

$$\mathrm{T_{xy}} = -\eta_l \frac{\partial v_x}{\partial y} \tag{4.2}$$

Assuming the fluid is semi-infinite, the surface mechanical impedance in Newtonian fluid is obtained by combining the Eq. (4.1), Eq. (4.2).

$$Z_{sys} = \left(\frac{\omega\rho_l\eta_l}{2}\right)^{\frac{1}{2}}(1+j) \tag{4.3}$$

Because the motional impedance is expressed in form of Eq. (4.3), surface stress becomes:

$$\sigma = \eta\frac{\partial v}{\partial y} = -(1+j)\frac{\eta}{\delta}v_s = -(1+j)\sqrt{\frac{\omega\eta\rho}{2}}v_s \tag{4.4}$$

The motion of equation under surface loading (especially Newtonian fluid) is:

$$\frac{E_H}{\rho}\frac{\partial^2 u}{\partial x^2} + D\frac{\partial u}{\partial t} - (1+j)\frac{2}{h}\frac{\eta}{\delta}\frac{\partial u}{\partial t} = \frac{\partial^2 u}{\partial t^2} \tag{4.5}$$

Because both sides of the resonator are immerged in fluid, the factor of the two is introduced in Eq. (4.5). And h means the thickness of the resonator. We know the general solution of Eq. (4.5), Eq. (4.5) may be simplified to:

$$\left[\omega_0^2 - \frac{2\eta}{h\rho\delta}\omega - \omega^2 + j\omega\left(D + \frac{2\eta}{h\rho\delta}\right)\right]u(x,t) = 0 \tag{4.6}$$

And the resonance frequency is approximated as follow:

$$\omega_0' = \omega_0\left(1 - \frac{1}{\rho h}\sqrt{\frac{\rho_l\eta_l}{2\omega_0}}\right) \tag{4.7}$$

Applying Eq. (4.7) to Eq. (3.29) and Eq. (3.30), we can get C_{nl}, R_{nl}.

$$C_{nl} = C_m^k \frac{1}{\rho h} \sqrt{\frac{\rho_l \eta_l}{2\omega_0}} \tag{4.8}$$

$$\frac{1}{R_{nl}} = \frac{1}{R_m^k} \frac{1}{\rho h} \sqrt{\frac{\rho_l \eta_l}{2\omega_0} Q} \tag{4.9}$$

4.3. Viscoelastic Loading

In ideal cases, material is assumed to purely elastic material or purely viscous material. But in reality, most of material possesses characteristics of both elastic and viscous material. These material is called viscoelastic material. Kelvin-Voigt model is commonly used for modeling viscoelastic materials such as viscous fluid [12].

1-DoF Kelvin-Voigt model for viscoelastic material is composed of a spring and a damper connected in parallel. The stress-strain relation in Kelvin-Voigt model is:

$$\sigma = E\epsilon + \eta_m \frac{\partial \epsilon}{\partial t} \tag{4.10}$$

where σ is the stress, ϵ is the strain and E and η_m are the elastic modulus and the viscosity coefficient of the medium, respectively. Under quasi-static harmonic excitation, the resulting 1-D wave equation becomes:

$$\frac{\partial^2 u}{\partial x^2} = \frac{\rho}{G^*} \frac{\partial^2 u}{\partial t^2} \tag{4.11}$$

where u is displacement of the particle, ρ is density of the medium, x is the propagation direction and $G^* = G' + jG''$ is the complex shear modulus [13].

The mechanical impedance of the viscoelastic loading may be written:

$$\widetilde{Z_{ve}} = -\frac{T_{xy}}{v_{p,x}}\bigg|_{y=0} = -\frac{G^*}{j\omega u_{x,o}} \frac{\partial u_{p,x}}{\partial y}\bigg|_{y=0} \tag{4.12}$$

Using Eq. (4.12) and Eq. (4.11), mechanical impedance due to a viscoelastic loading is:

$$\widetilde{Z_{ve}} = \sqrt{\rho_l G^*} \tanh(\gamma h_l) \text{ where } \gamma = j\omega \sqrt{\frac{\rho_l}{G^*}} \tag{4.13}$$

Where $\widetilde{Z_{ve}}$ is mechanical impedance of viscoelastic loading. Using approximation, Eq. (4.13) is approximated as follows.

$$\tanh(\gamma h_l) \cong \frac{8\gamma h_l}{(N'\pi)^2 + (2\gamma h)^2} \tag{4.14}$$

where N' is the harmonic number. Taking lowest-harmonics ($N' = 1$) and substitute Eq. (4.14) into Eq. (4.13) gives following approximation for the motional electrical impedance arisen from viscoelastic load.

$$Z_{ve} \cong \left[\frac{\omega h_l G''}{2|G^*|^2} + j\omega\left(\frac{h_l G'}{2|G^*|^2}\right) + \frac{1}{j\omega}\left(\frac{\pi^2}{8h_l\rho_l\pi}\right)\right]^{-1} = R_{ve} + jX_{ve} \tag{4.15}$$

4.4. Maxwellian Fluid Loading

Maxwellian fluid is specific type of non-Newtonian, viscoelastic fluid that considers the finite reorientation time of molecules under shear stress. The fluid exhibits a 1st order relaxation process [14].

$$\eta(\omega) = \frac{\eta_0}{1 + j\omega\tau} \tag{4.16}$$

where η_0 is the static shear viscosity on low-frequency condition and τ is the relaxation time. Maxwellian fluid exhibits viscoelastic behavior. The Maxwellian fluid analyze three parts. First of all, when the strain rate is low ($\omega\tau \ll 1$), the Maxwellian fluid behaves as a Newtonian fluid. However, when $\omega\tau$ approaches 1 ($\omega\tau \approx 1$), the elastic energy is not totally dissipated and some of the energy is stored elastically. In contrast, when $\omega\tau \gg 1$, the fluid behaves as an elastic solid.

The equation of motion of the Maxwellian fluid is identical to that of Newtonian fluid except complex propagation factor γ. γ of the Maxwellian fluid is defined as following.

$$\gamma^2 = \frac{j\omega\rho_l}{\eta_0}(1 + j\omega\tau) \tag{4.17}$$

Then, substituting equations in a fashion similar to that used for the Newtonian fluid gives mechanical impedance of Maxwellian fluid.

$$\widetilde{Z_{mx}} = \sqrt{\frac{j\omega\rho_l\eta_0}{1 + j\omega\tau}} \tag{4.18}$$

Resistance and reactance part of the Maxwellian fluid can be obtained from Eq. (4.18).

$$R_{mx} = \frac{1}{R_m}\frac{1}{\rho h}\sqrt{\frac{\rho_l \eta_l}{2\omega_0}Q}\sqrt{1 - \frac{\omega\tau}{\sqrt{1+(\omega\tau)^2}}}\sqrt{\frac{1}{\sqrt{1+(\omega\tau)^2}}} \tag{4.19}$$

$$C_{mx} = C_m\frac{1}{\rho h}\sqrt{\frac{\rho_l \eta_l}{2\omega_0}}\sqrt{1 + \frac{\omega\tau}{\sqrt{1+(\omega\tau)^2}}}\sqrt{\frac{1}{\sqrt{1+(\omega\tau)^2}}} \tag{4.20}$$

4.5. Equivalent electrical circuit under surface loading

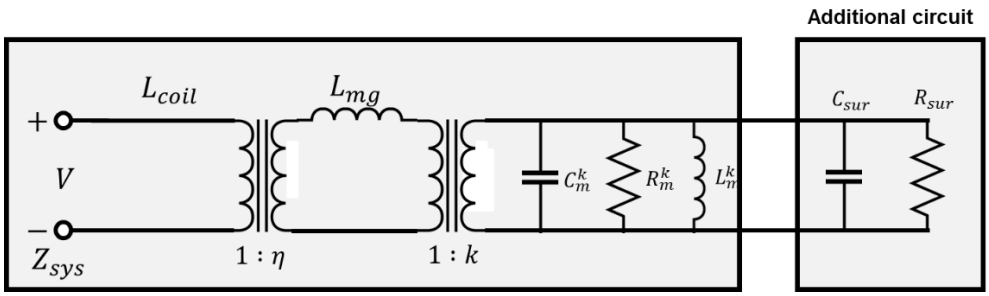

Figure 4.1 Equivalent electrical circuit under surface loading

Figure 4.1 depict the equivalent electrical circuit under surface loading. This circuit is almost same with equivalent circuit in air. One thing different is additional parallel circuit. Additional circuit contains capacitance and resistance under surface loading. This is so powerful that any kind of surface loading can be added with parallel circuit. C_{sur} and R_{sur} are can be calculated from 4.1 ~ 4.4 in Chapter 4.

CHAPTER 5.

EXPERIMENTAL RESULTS IN AIR

In this section, the modeling of the resonator in Chapter 3 is verified with experimental data. After the result of experiments in air is discussed, the result of experiments in viscous liquid is mentioned.

5.1. Experimental Setup

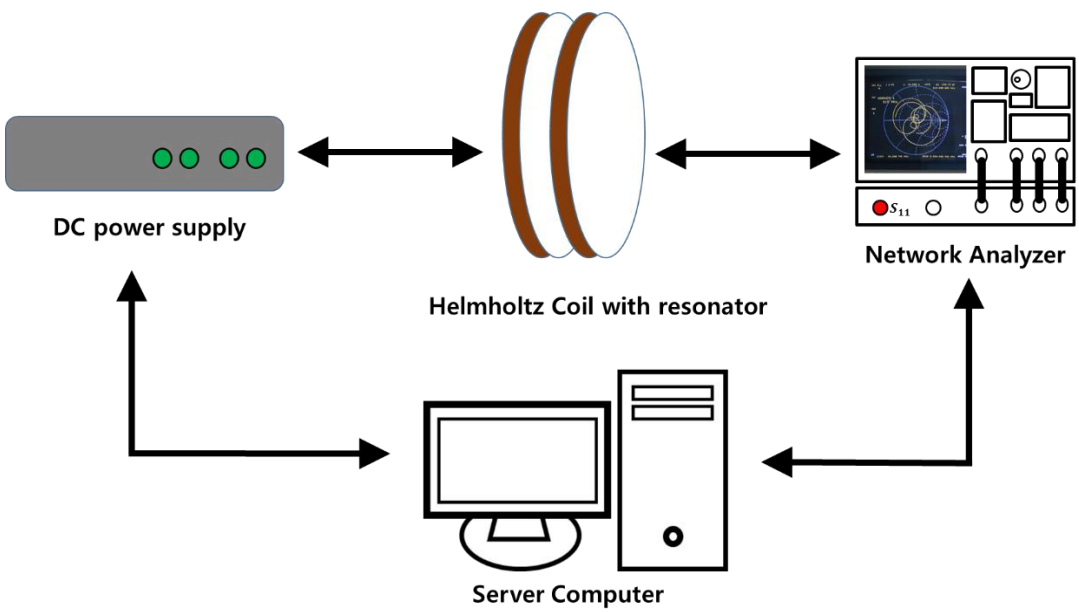

Figure 5.1 Schematic diagram of experimental setup

Figure 5.1 is the schematic of the experimental setup. The system in this paper is consist of 4 parts which are DC power supply, Helmholtz coil, Network Analyzer and Server computer. Because DC power supply is programmable, a DC bias field is controlled by server computer. A DC bias field is in range of 1A in this paper, but 0.3A, which is maximum efficiency, is mainly used. This fact is proved in section

5.1. The Helmholtz coil is consist of pair of DC coil with radius of 50mm to provide uniform DC bias field. The resonator is placed in Helmholtz coil and the resonator used in this paper is Metglas™ 2826MB which thickness is 30*um*. 2826MB is ferromagnetic material and no field annealing or surface treatment was done. Resonator is excited with an AC magnetic field and AC field is generated by a vector network analyzer (HP8751A) which consists of 801 number of points while frequency sweeping. 4.4

Table 5.1 Resonator setup in experiments. All units are in *mm*

Resonator number	Geometry ($\boldsymbol{w} \times \boldsymbol{h} \times \boldsymbol{l}$)	Aspect Ratio (l/w)
1	5.2 x 0.03 x 20	0.26
2	4.4 x 0.03 x 17	0.26
3	3.64 x 0.03 x 14	0.26
4	2.9 x 0.03 x 11	0.26

Geometries of resonator for experiments are listed in Table 5.1. Geometry of a resonator is related to its resonant frequency, response magnitude. Resonant frequency is arranged in the range of 100-110 *kHz*. Because it is well known that longitudinal resonant frequency is affected by length of the resonator, 4-types of resonator are chosen in this experiments. Although all resonators have different length, all resonator have same aspect ratio. Aspect ratio of the resonator have an influence on demagnetizing factor, resonant mode of the resonator and relative surface area of the resonator. Because demagnetizing factor, resonant mode, relative surface area may induce distortions in resonator responses, all resonator is arranged with same aspect ratio.

5.2. Effect of DC Bias Field

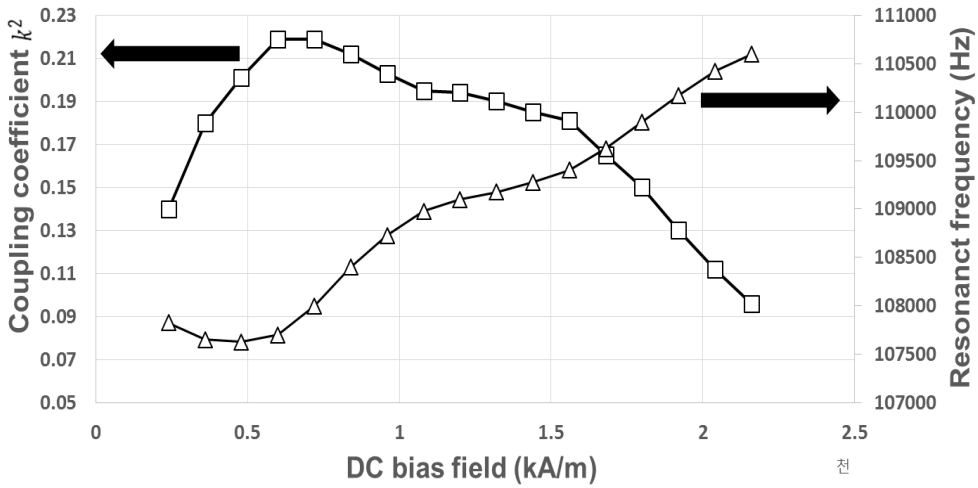

Figure 5.2 Magnetoelastic coupling coefficient k^2 and resonant frequency $f_0$of resonator (w x l = 5.2mm x 20mm) as a function of DC bias field

Figure 5.2 illustrates magnetoelastic coupling factor k^2 and resonant frequency is a function of DC bias field. Magnetoelastic coupling coefficient which means efficiency of magnetic-to-elastic conversion, vice versa, reaches maximum value at 1000A/m. Therefore, by definition in Eq. (2.14), the resonator has maximum conversion efficiency between the magnetic energy and the elastic energy nearby 1000A/m. Figure 5.2 also shows that the resonant frequency f_0 reaches minimum value at maximum magnetoelastic coupling factor. Because the resonance frequency is a function of Young's modulus ($f_0 = 1/2L(E/\rho)^{0.5}$), the resonant frequency reaches its minimum value at maximum k^2 value. As mentioned in 2.2 ΔE Effect, resonance frequency is changed because k^2 have a direct influence on Young's modulus of the resonator. It is important that k^2 is not associated with geometry of resonator. Susceptibility and effective Young's Modulus is basically intrinsic

properties of the material in Eq. (2.18), so k^2 is nearly same if the resonator is composed of same material. In other words, k^2 is independent with geometry of resonator.

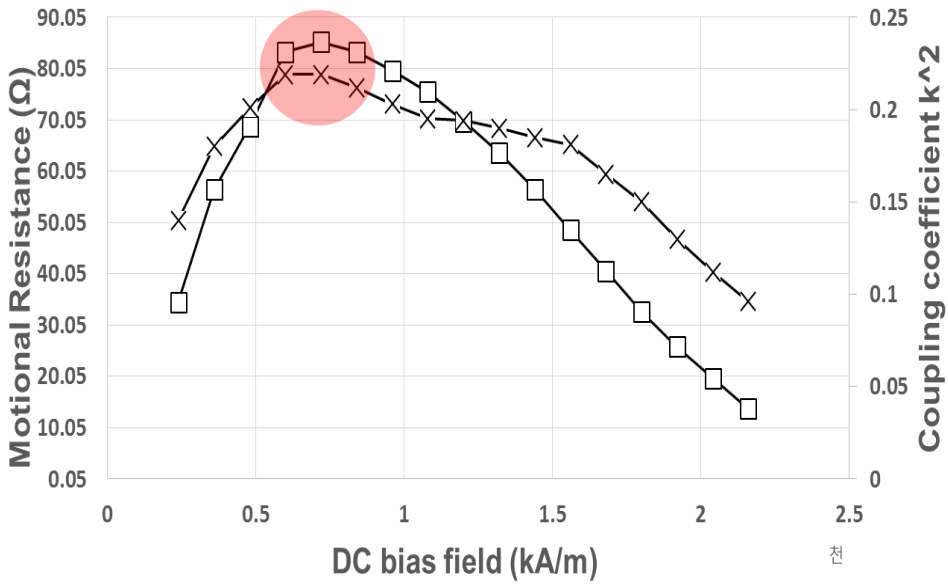

Figure 5.3 Motional Resistance R_m of resonator (w x l = 5.2mm x 20mm) as a function of DC bias field

Figure 5.3 shows that motional resistance R_m also has maximum value at maximum magnetoelastic coupling factor k^2. Because k^2 is magnetic-to-elastic energy conversion ratio, k^2 have an effect upon motional resistance. Because motional resistance has same value with impedance of resonator at resonance, it is natural that the magnitude of resonator has same tendency of magnetoelastic coupling factor. This phenomenon is also verified by Eq. (3.29). In Eq. (3.29), motional resistance has an direct proportion relation with k^2, so shape of both graph are similar.

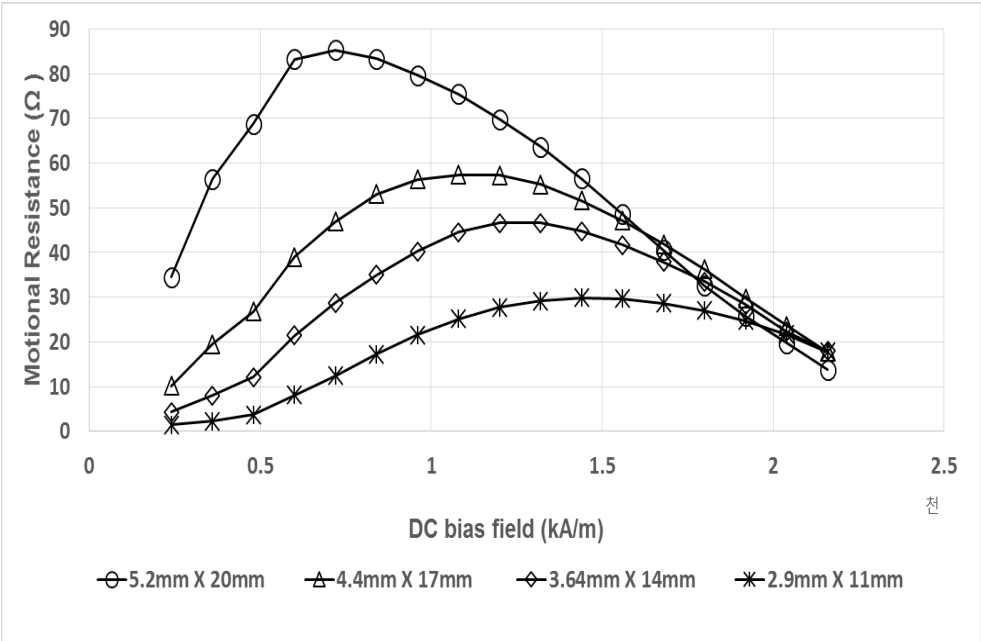

Figure 5.4 Motional Resistance R_m of four-types of resonator which have same aspect ratio as a function of DC bias field

Figure 5.4 shows measured motional resistance of four-types of resonator. In order to compare the effect of resonator size, all resonator are arranged with same aspect ratio. As shown in Figure 5.4, the magnitude of resonator is related to geometry of resonator. This results indicates that the bigger resonator is, the larger magnitude is. This phenomenon is verified by Eq. (3.26). By Eq. (3.26), magnitude of resonator is proportional to area of resonator, not an width and length. So 5.2mm X 20mm resonator has larger magnitude than the other resonator.

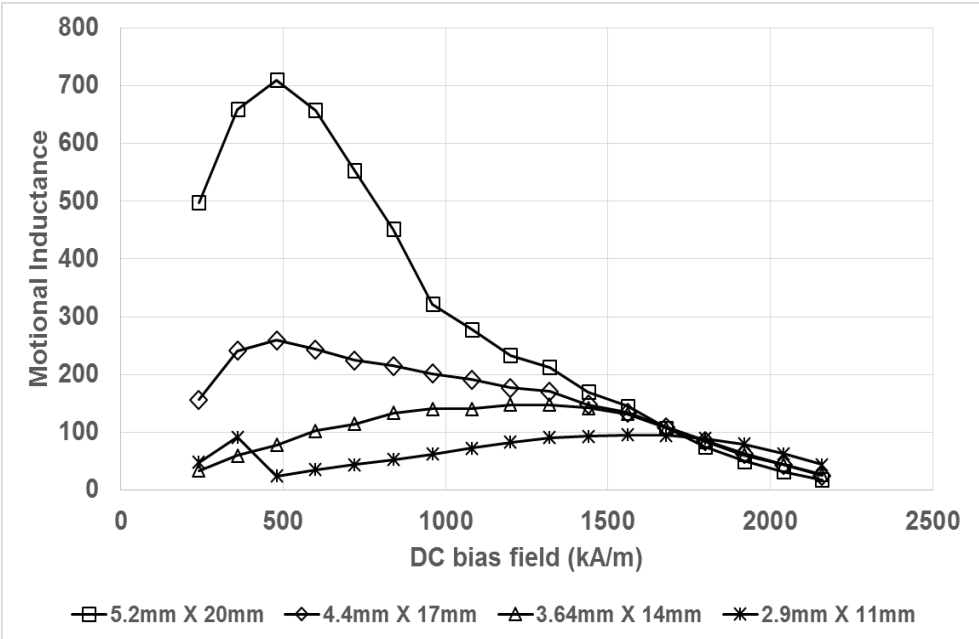

Figure 5.5 Motional inductance L_m of four-types of resonator which have same aspect ratio as a function of DC bias field

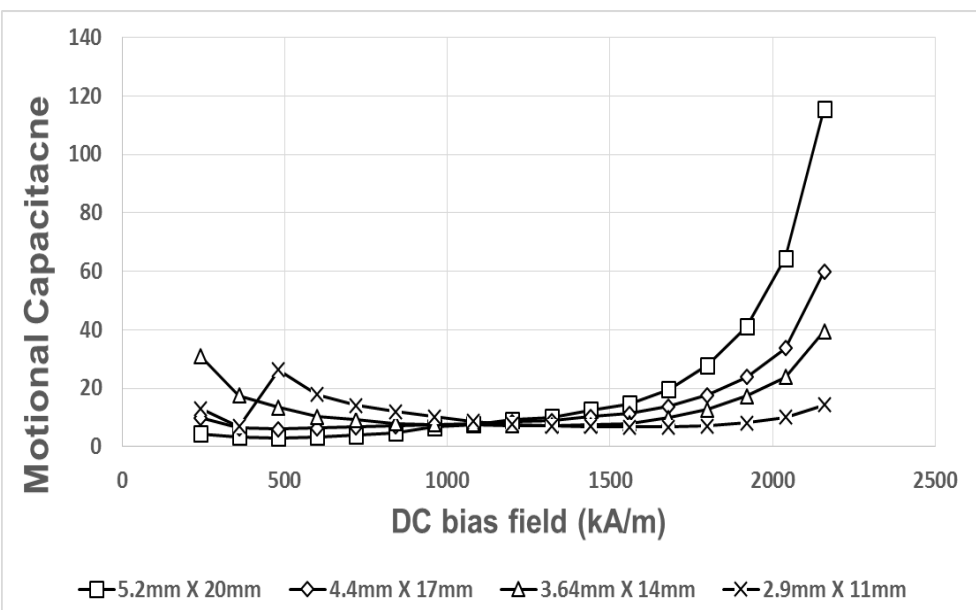

Figure 5.6 Motional capacitance C_m of four-types of resonator which have same aspect ratio as a function of DC bias field

Figure 5.5 and Figure 5.6 are motional capacitance C_m and motional inductance L_m of the resonator respectively. In order to compare the effect of resonator size, all resonator are arranged with same aspect ratio. In Eq. (3.28), motional inductance is proportional to coupling coefficient, so motional inductance has same tendency of magnetoelastic coupling factor. In Eq. (3.28) and Eq. (3.30), motional capacitance is reciprocal proportion to motional inductance, it is confirmed by Figure 5.5 and Figure 5.6.

CHAPTER 6.EXPERIMENTAL RESULT IN VISCOUS LIQUID

In this section, the modeling of the resonator in Chapter 4 is verified with experimental data.

6.1. Experimental Setup

In this section, responses of the resonator according to the change of viscosity are discussed. Basic experimental setup is same with Figure 5.1. Since responses of the resonator according to the change of viscosity are important, all experiments are executed in same resonator. Because the 5.2mm X 20mm resonator has biggest response as mentioned in Chapter 4, 5.2mm X 20mm resonator is used in this section.

To control the kinematic viscosity, KF-96 which has exact kinematic viscosity and density is used. Table 6.1 is the specification of KF-96 and 11 kinds of KF-96 are used.

Table 6.1 KF-96 specifications

Kinematic viscosity	specific gravity
1.5	0.852
5	0.915
10	0.935
20	0.95

30	0.95
50	0.96
100	0.965
200	0.97
300	0.97
350	0.97
500	0.97

6.2. Effect of viscosity

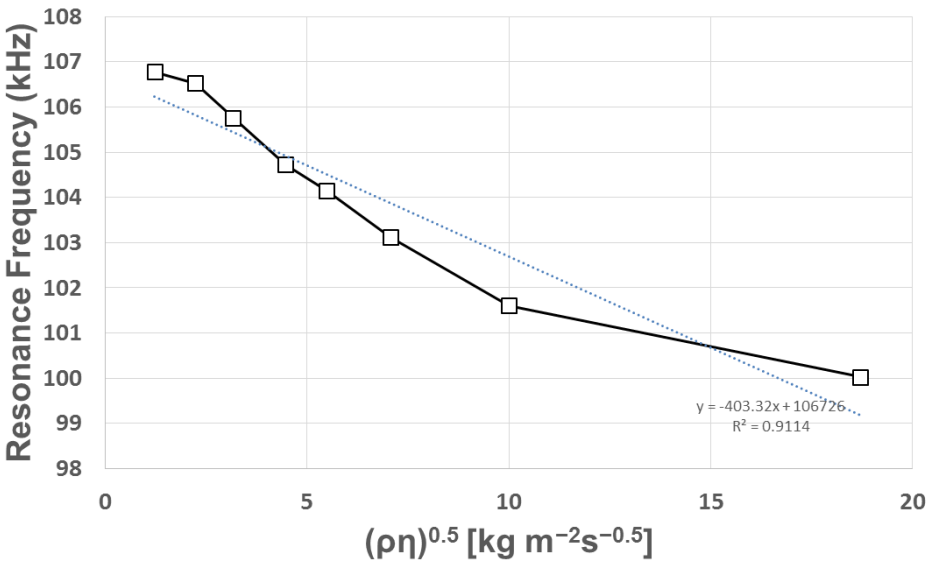

Figure 6.1 Resonance frequency shift according to the change of kinematic viscosity. (Resonator = 5.2mm X 20mm, KF-96)

Figure 6.1 shows the resonance frequency shift according to the change of kinematic viscosity. η means the dynamic viscosity and $(\rho\eta)^{0.5}$ of the x-axis means the kinematic viscosity. It is quite clear that the higher the kinematic viscosity is, the more resonant frequency shifts. From Eq. (4.7):

$$\omega_0' \propto \sqrt{\rho_l \eta_l} \tag{6.1}$$

In Eq (6.1), resonant frequency is proportional to $(\rho\eta)^{0.5}$, so the graph above is linear expression.

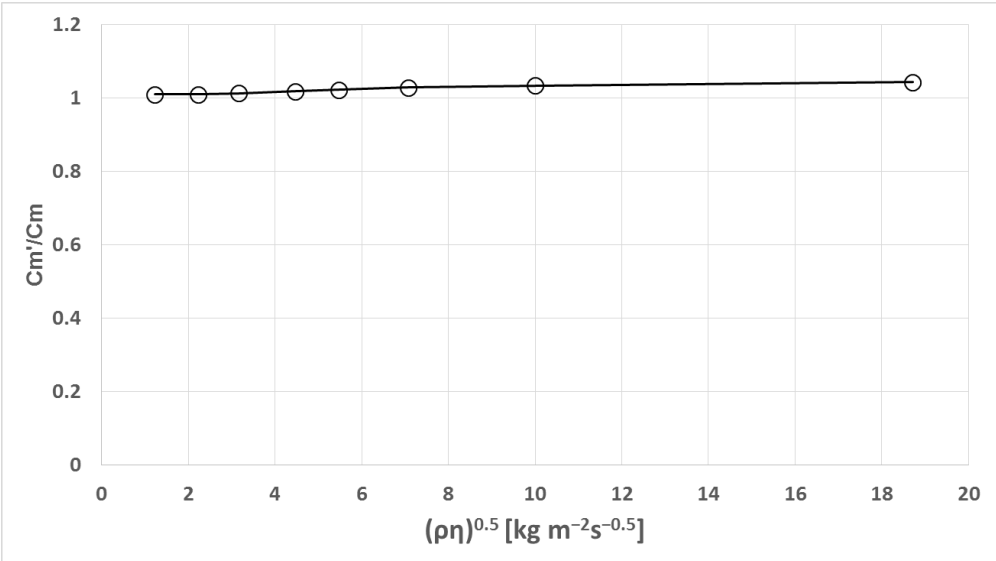

Figure 6.2 Ratio of motional capacitance under surface loading with respect to $\sqrt{\rho_l \eta_l}$.

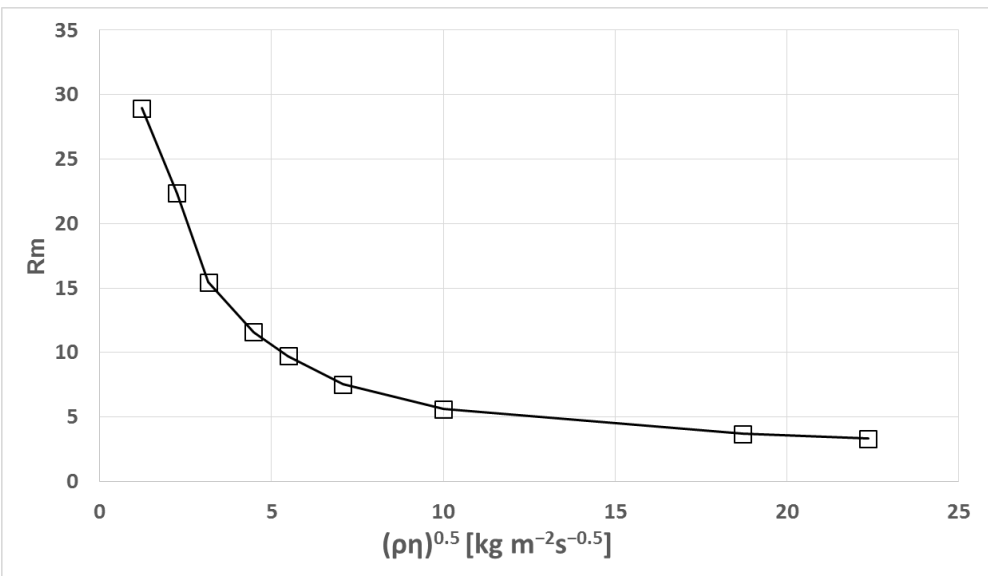

Figure 6.3 Motional resistance Rm under surface loading with respect to $\sqrt{\rho_l \eta_l}$.

Figure 6.2 shows comparison between calculated motional capacitance and measured motional capacitance under viscous loading. From Eq.(4.8):

$$\frac{C_{nl}}{C_m^k} = 1 + \frac{1}{\rho h}\sqrt{\frac{\rho_l \eta_l}{2\omega_0}} \tag{6.2}$$

As shown in Eq. (6.2), motional capacitance is also proportional to $(\rho\eta)^{0.5}$ and motional capacitance can be calculated according to the change of $(\rho\eta)^{0.5}$. In Figure 6.2, motional capacitance is calculated from resonant frequency and $(\rho\eta)^{0.5}$. Because the value of **Cm'/Cm** is almost 1, so the calculated motional capacitance is accurate. In fact, the error is 4%. Because Lm and Cm have following relation:

$$f_r = \frac{1}{2\pi\sqrt{L_m C_m}} \tag{6.3}$$

Motional inductance of the resonator under surface loading can be calculated from motional capacitance.

Figure 6.3 indicate the ratio of motional resistance under surface loading.

$$\frac{R_m}{R_{m'}} = 1 + \frac{1}{\rho h}\sqrt{\frac{\rho_l \eta_l}{2\omega_0} Q} \tag{6.4}$$

In Eq. (6.4), motional resistance under surface loading R_m' is a reciprocal proportion to $(\rho\eta)^{0.5}$, thus increasing kinematic viscosity lead to decreasing motional resistance.

CHAPTER 7.
CONCLUSION

This paper introduces an equivalent electrical circuit model in air for magnetoelastic resonator system. The whole system are expressed with impedance Z including AC excitation coil, coupling factor, demagnetizing factor, magnetization of material and magnetization. Especially, coupling factor and demagnetizing factor are depicted as a transformer winding ratio η and k repectively.

Also in this paper, an equivalent circuit in viscous loading is introduced. As explanation in Chapter 4.5, additional circuit can be added directly to magnetoelastic resonator model without modifying the model. Furthermore, when various surface loading is applied simultaneously to the magnetoelastic resonator, adding equivalent circuit in series describes the behavior of the resonator.

The case studies based on magnetoelastic resonator operating at several geometries, DC field condition and kinematic viscosity are discussed for verification of suitability of the proposed modeling for describing behavior or magnetoelastic resonator system.

REFERENCES

[1] S. W. W. a. R. M. W. B. A. Martin, Viscosity and density sensing with ultrasonic plate waves, Sensors Actuators A Phys, 1989.

[2] U. B. K. L. a. B. T. B. Derjaguin, Shear elasticity of low-viscosity liquids at low frequencies, Phys. Rev. A, vol. 42, no. 4, pp. 2255–2258, 1990.

[3] A. J. V. F. W. V. a. S. M. W. J. C. Butler, Wireless, passive, resonant-circuit, inductively coupled, inductive strain sensor, Sensors Actuators A Phys, vol. 102, no. 1–2, pp. 61–66, 2002.

[4] S. Schodowski, Resonator self-temperature-sensing using a dual-harmonic-mode crystal oscillator, Freq. Control, 1989.

[5] B. C. a. C. Graham, Introduction to Magnetic Materials, John Wiley & Sons, 2008.

[6] R. C. S. ,. L. E. F. A. B. F. by Marcelo J. Dapino, A coupled structural-magnetic strain and stress model for magnetostrictive transducers, J. Intell, 2000.

[7] A. E. C. H. J. S. R. J. A. M. A. Mitchell, ΔE effect and magnetomechanical coupling factor in Fe80B20 and Fe78Si10B12 glassy ribbons, IEEE Trans. Magn., vol. M, no. 12, p. 1170, 1978.

[8] T. O'Dell, Measurement of magnetomechanical coupling factor in amorphous ribbons, Phys. status solidi, vol. 565, pp. 565–572, 1982.

[9] U. F. Gianola, Application of the Wiedemann Effect to the Magnetostrictive Coupling of Crossed Coils, . Appl. Phys., vol. 26, no. 9, p. 1152, 1955.

[10] K. G. O. K. L. P. G. S. D. K. Y. L. C. T. a. F. T. C. A. Grimes, Magnetoelastic sensors for remote query environmental monitoring, Smart Mater. Struct., vol. 8, no. 5, pp. 639–646, 1999.

[11] I. K. K. a. Y. Y. Kim, Shear horizontal wave transduction in plates by magnetostrictive gratings, J. Mech. Sci. Technol., vol. 21, no. 5, pp. 693–698, 2007.

[12] B. C. a. C. Graham, Introduction to magnetic materials, 2011.

[13] A. E. C. a. M. Wun-Fogle, A new method of magnetostrictivity and magnetostriction measurement - Magnetics, IEEE Transactions on, IEEE Trans. Magn., vol. 25, no. 5, pp. 3611–3613, 1989.

[14] S. J. M. R. W. C. a. A. R. H. H. L. Bandey, Modeling the Responses of Thickness-Shear Mode Resonators under Various Loading Conditions, Anal. Chem., vol. 71, no. 11, pp. 2205–14, 1999.